A&A 377, L27–L30 (2001)
DOI: 10.1051/0004-6361:20011211

Astronomy & Astrophysics

Letter to the Editor

The interpretation of Mn II emission from late-type B stars

T. A. A. Sigut⋆

Department of Physics and Astronomy, The University of Western Ontario, London, Ontario, Canada N6A 3K7

Received 12 March 2001 / Accepted 29 August 2001

Abstract. The photospheric Mn II emission lines Wahlgren & Hubrig (2000) detect in the spectra of several late-type B and HgMn stars and attribute to fluorescent excitation are more naturally explained by interlocked non-LTE effects acting in a photosphere in which the manganese abundance is stratified with depth. The case is particularly strong for HD 186122 (46 Aql) and HD 179761 both of which require the manganese overabundance to be concentrated to column masses of $\log(m) < \approx -1.5$.

Key words. line: formation – radiative transfer – stars: chemically peculiar, emission-line, Be

1. Introduction

Stellar emission lines are usually interpreted as evidence for a chromospheric temperature rise, mass outflow, or the presence of circumstellar material. However, emission lines from "classical" stellar photospheres, in which none of the previous mechanisms operate, cannot be ruled out a priori as the specific intensity in a transition is determined by a source function which may respond in a complex way to the presence of non-local sources and sinks of line photons. Examples of this caveat are the photospheric emission lines of Mn II multiplet 13 ($\lambda\lambda 6122 - 6132$ Å, $4d\,^5D \rightarrow 4f\,^5F^o$) recently detected in the spectra of the ^{3}He star 3 Cen A (HD 120709, B5 III-IVp) and the hot, mild, HgMn star 46 Aql (HD 186122, B9 III) by Sigut et al. (2000). Sigut (2001) has demonstrated that these emission lines can arise via inter-locked non-LTE effects which decouple the line source function from the local Planck function and result in a line source function which rises with photospheric height. It was also argued that an essential ingredient in reproducing the *strength* of the observed manganese emission within the non-LTE framework is a stratification of the manganese abundance profile in the photosphere, concentrating the manganese in a layer at small column mass.

Recently, Wahlgren & Hubrig (2000, W&H hereafter) have also detected weak emission from Mn II multiplet 13, as well as from additional transitions of Cr II and Ti II, in the red spectra of several late-type B and HgMn stars. W&H postulate selective excitation via Lyα fluorescence as the emission mechanism. In this letter, it is demonstrated that the Mn II emission detected by W&H is consistent with the non-LTE excitation mechanism of Sigut (2001). Specific stratification models for each star are proposed as constrained by the available observations. The possible role of Lyα fluorescent excitation is also discussed.

2. Calculations

The coupled equations of radiative transfer and statistical equilibrium for Mn II were solved with the MULTI code, v2.0, of Carlsson (1992). Solutions were obtained in model photospheres appropriate for the seven late-B and HgMn stars for which W&H list Mn II multiplet 13 ($4d\,^5D_4 \rightarrow 4f\,^5F^o_5$, $\lambda\,6122.4$ Å) equivalent widths (see Table 1). For each star, the $T_{\rm eff}$ and $\log(g)$ adopted by W&H were used, and each model photosphere was represented by an Kurucz LTE model atmosphere. Direct comparison to non-LTE model atmospheres (Grigsby 1991; Grigsby et al. 1992) and to observed UV-to-optical spectral energy distributions (Fitzpatrick & Massa 1999) demonstrates that the approximation of LTE model atmospheres is a reasonable one for this range of stellar parameters.

The Mn II model atom consisted of 84 total $LS\pi$ multiplet levels from the quintet and septet symmetries. The atomic data used was the same as that described in Sigut (2001). To obtain a realistic assessment of the uncertainties in the non-LTE predictions due to the large uncertainties in the basic atomic data, Monte Carlo simulations were performed. Generous errors were assigned to all of the atomic data (see Sigut 2001), and 15 sets of Mn II atomic data were realized and used in the non-LTE calculations. This gave, for each model photosphere and stratification model, 15 estimates of the equivalent width of each Mn II transition, and the standard deviation in these values was taken as an estimate of the uncertainty. The use of Monte Carlo simulation to estimate the errors in non-LTE calculations is discussed by Sigut (1996).

⋆ e-mail: asigut@despot.astro.uwo.ca

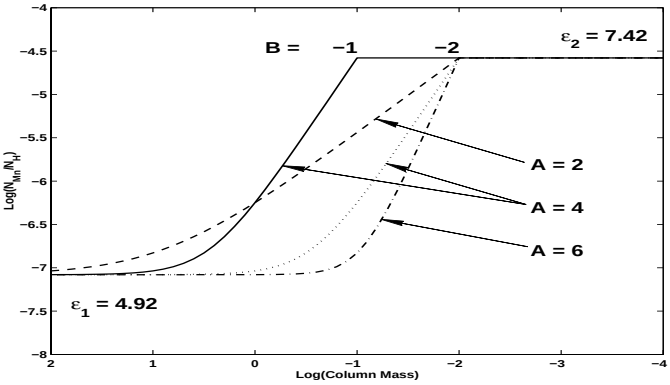

Fig. 1. The two-zone stratification model for the manganese abundance for several choices of the model parameters.

Stratification of the manganese abundance profile with photospheric depth was represented by a simple two-zone model depending on four parameters: the manganese abundance in the lower zone (ϵ_1), the manganese abundance in the upper zone (ϵ_2), the location in column mass of the transition between the two zones (B), and a parameter setting the sharpness of the transition between the zones (A). In terms of these parameters, the particle conservation equation at each depth was written as

$$\sum_{i=1}^{N_{\rm L}} (N_i/N_{\rm H}) = 10^{(\epsilon_2-12)}\, {\rm e}^{-A\,(\log\, m - B)} + 10^{(\epsilon_1-12)}\,, \qquad (1)$$

for $\log\, m \geq B$, and

$$\sum_{i=1}^{N_{\rm L}} (N_i/N_{\rm H}) = 10^{(\epsilon_2-12)} + 10^{(\epsilon_1-12)}\,, \qquad (2)$$

for $\log\, m < B$. Here $N_{\rm H}$ is the hydrogen number density, $N_{\rm L}$ the number of Mn II/Mn III levels included in the non-LTE solution (namely 85), and m is the photospheric column mass. Figure 1 illustrates this simple, two-zone model for some representative choices of the parameters.

3. Results

The calculated non-LTE Mn II equivalent widths for various stratification models were compared to the late B-star observations of W&H. The zone abundances, ϵ_1 and ϵ_2, were independently varied from 2.92 to 7.92 in steps of 0.5 dex[1]. Only models with an overabundance in the upper zone ($\epsilon_2 > \epsilon_1$) were considered, aside from a reference grid of unstratified models covering the same abundance range. Parameter B, which determines the location of the transition between the zones, was assumed to have values of -1.0, -1.5, or -2.0. Models with $B > -1$ gave predictions which differed little from unstratified models of abundance ϵ_2 because the zone boundary is near or below the depth of formation of multiplet 13. Parameter A, governing the sharpness of the transition between the two zones, was assumed to have values of 2, 4, or 6. As can be seen from Fig. 1, larger values for parameter A give a sharper transition between the two abundance zones.

[1] The solar manganese abundance is $\epsilon = 5.39$ dex (Anders & Grevesse 1989).

Table 1. Unstratified models for the late-B stars of W&H.

HD	$T_{\rm eff}$, log(g)	[Mn/H]	W_λ	ϵ Range	$W_\lambda^{\rm calc}$
209459	10 350, 3.48	+0.25	+1.4	5.5−5.8	5.0 ± 0.25
186122	12 910, 3.74	+0.80	−2.9	6.4−6.8	15.5 ± 1.3
196426	13 010, 3.84	+0.25	−1.4	5.8−6.1	2.7 ± 0.75
179761	13 030, 3.43	+0.80	−1.6	6.3−6.7	13.0 ± 1.1
186568	11 700, 3.50		−0.9	4.4−5.2	
219927	12 970, 3.63		−1.2	4.4−5.6	
16727	14 500, 4.19		−0.6	[a]4.4−4.7	
				[b]5.6−6.0	

Notes.- The stellar parameters, manganese abundance, and $\lambda\,6122.4$ Å equivalent width (W_λ, in mÅ) are adopted from W&H. The interpretation of ϵ-Range is different for stars without [Mn/H] values – see text for details. There are two matching ranges for HD 16727, labeled (a) and (b).

Given these parameters, acceptable stratification models for each star were chosen to reproduce two observations: (1) the strength of Mn II multiplet 13, $W_\lambda(\lambda\,6122.4)$, and (2) the photospheric manganese abundance determined by previous workers, [Mn/H]. The form of the second constraint stems from the fact that none of the available abundance studies for the stars of Table 1 provide equivalent widths for manganese. Therefore, the manganese abundances derived by these studies were assumed to parameterize the strengths of the weak, optical, Mn II transitions used. To implement the constraint [Mn/H], an LTE abundance analysis was performed on the *predicted non-LTE equivalent width* of $\lambda\,4326$ (Mn II a ^{5}F$_4$ → z ^{5}F$_4$) in each stratification model. This generally weak, visible line is typical of those used in the abundance analysis of manganese. The hyperfine structure of $\lambda\,4326$ was explicitly included in both the LTE and non-LTE calculations using the experimental measurements of Holt et al. (1999). A probable error of ±15% was assigned to the $W_\lambda(\lambda\,6122.4)$ data of W&H, and ±0.20 dex to the various LTE manganese abundance determinations. As noted by Sigut et al. (2000), the oscillator strength of $\lambda\,6122.4$ is unlikely to be in error by a large amount.

3.1. Unstratified models

Table 1 summarizes an analysis of the W&H stars using models with a uniform manganese abundance as a function of photospheric depth. For the four stars with available [Mn/H], Table 1 gives the (unstratified) manganese abundance range (under column "ϵ Range") for which the LTE abundance required to match the computed non-LTE equivalent width of $\lambda\,4326$ matches the literature value within ±0.2 dex. The next column, $W_\lambda^{\rm calc}$, gives the *predicted* non-LTE equivalent width of $\lambda\,6122.4$,

along with its 1σ error, for a manganese abundance at the midpoint of this range. In all cases, the unstratified models which match the LTE manganese abundance *fail by large amounts* to explain the strength of the $\lambda\,6122.4$ emission. The closest match is for HD 196426 where the calculated $\lambda\,6122.4$ strength differs from the observed value by over 5 standard deviations. The remaining stars all differ by more than 10 standard deviations. Thus unstratified models are unable to simultaneously match both constraints, prompting stratified models to be considered in the next section.

For the three remaining stars, the constraint of [Mn/H] is unavailable, and it is not possible to rule out unstratified models. In this case, the column "ϵ Range" reports the range of manganese abundances for which the predicted equivalent width of $\lambda\,6122.4$ matches the observed value within the combined observational and theoretical errors. The range of abundances found are generally solar to subsolar.

One possible strategy to salvage unstratified models is to assume that the $T_{\rm eff}$ and $\log(g)$ values for the stars are in error by large amounts. For the two stars with large manganese overabundances relative to the sun, HD 186122 (46 Aql) and HD 179761, it was not possible to find unstratified models matching both constraints within ±1000 K in $T_{\rm eff}$ and ±0.25 dex in $\log(g)$. However, for the two remaining stars with only modest manganese overabundances, matching unstratified models could be found. A model with $T_{\rm eff} = 14\,000$ K and $\log(g) = 3.5$ can reproduce the HD 196426 observations for the narrow abundance range of $\epsilon = 5.9 - 6.0$ dex. For HD 209459, a model with $T_{\rm eff} = 11\,500$ K and $\log(g) = 3.5$ can reproduce the observations for the abundance range of $\epsilon = 5.6$–5.7 dex. However, the errors in $T_{\rm eff}$ implied in both cases are $\approx$1000 K and are at the outer limit of plausibility (Adelman & Rayle 2000). For this reason, stratified models for these two stars have also been investigated.

3.2. Stratified models

Given the failure of unstratified models to reproduce the observations, particularly for HD 186122 (46 Aql) and HD 179761, stratified models were considered. Figure 2 presents the results for 46 Aql. Each panel in the figure represents a single choice of the parameters B (location of the zone transition) and A (sharpness of the zone transition). Given the (B, A) values, a square is plotted in the (ϵ_1, ϵ_2) plane if that stratified model can reproduce the [Mn/H] abundance within ±0.2 dex, and an open circle is plotted if that stratified model can reproduce the strength of $\lambda\,6122.4$ within the combined theoretical and experimental errors. Thus a consistent stratified model is represented by a circle containing a filled square. For 46 Aql, only models with $B = -1.5$ and $A = 6$ or $B = -2.0$ and $A \geq 4$ give consistent results. This occurs for an upper zone abundance in the range of $\epsilon_2 \approx 6.8$–7.5 although the exact value depends on the chosen (B, A) parameters. The lower zone abundance is less well defined with matching models generally occurring for $\epsilon_1 < \approx 5.0$.

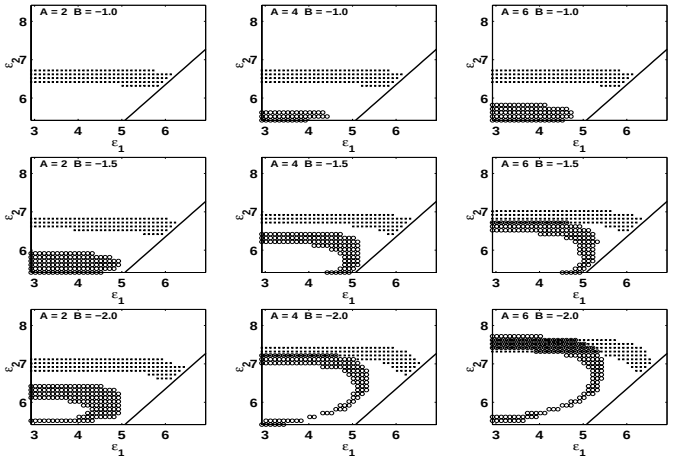

Fig. 2. Stratified models for HD 186122 (46 Aql). The (A, B) parameters of Eqs. (1) and (2) are indicated in each panel. As described in the text, viable stratified models only occur in the overlap region of the circles and filled squares. All models in the (ϵ_1, ϵ_2) plane were considered except those below and to the right of the solid line.

Figure 3 summaries the matching stratification models for the three remaining stars with both multiplet 13 equivalent widths and [Mn/H] abundances. In this figure, a symbol is plotted in the (ϵ_1, ϵ_2) plane only if that model matches both constraints, *unlike* Fig. 2. For HD 179761, which like 46 Aql has a large [Mn/H] enhancement, matching models are only found for $B \leq -1.5$ and $A \geq 4$ with $\epsilon_2 \approx 7.0 - 8.0$ and $\epsilon_1 < \approx 5.5$. However, for the two remaining stars with only moderate manganese overabundances, a wide variety of stratification models can match the observations.

4. Lyα fluorescent excitation of multiplet 13?

W&H suggest an alternative origin for the Mn II emission lines, namely Lyα fluorescent excitation with the Mn II emission formed by population cascade as in a photoionized nebula. W&H note close wavelength co-incidences between transitions in the Mn II term system and Lyα, most notably those connecting the ground state with the lower level of multiplet 13, $4{\rm d}\,^5{\rm D}$, and those connecting the low-lying meta-stable state a^5D with the upper level of multiplet 13, $4{\rm f}\,^5{\rm F^o}$. Seductive as these close overlaps may be, wavelength coincidence alone is not sufficient for fluorescent excitation. Consider a weak, Mn II transition with line profile $\phi_{ij}^{\rm Mn}$ within $\delta\nu$ of Lyα. The net excitation rate in this transition due to Lyα is

$$R(i \rightarrow j) = n_i\, B_{ij} \bar{J} - n_j (A_{ji} + B_{ji} \bar{J})\,, \qquad (3)$$

where

$$\bar{J} = \int \phi_{ij}^{\rm Mn}\, J_\nu\, {\rm d}\nu = \Lambda[S^{\rm Ly\alpha}]\,. \qquad (4)$$

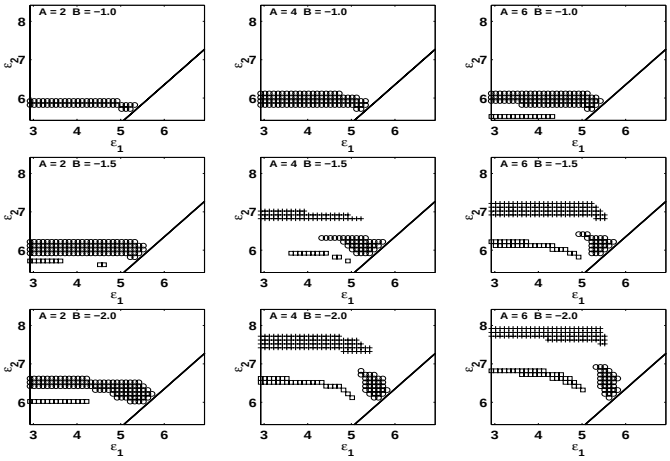

Fig. 3. Matching stratification models for HD 209459 (squares), HD 196426 (circles), and HD 179761 (crosses). Unlike Fig. 2, each symbol represents a viable stratification model.

$S^{\mathrm{Ly}\alpha}$ is the Lyα source function, and Λ is the Λ-operator representing, in integral-operator form, the formal solution to the transfer equation. The second step in Eq. (3) assumes that Lyα will dominate the radiation field at this frequency and that J_ν is sensibly constant over the narrow range of $\delta\nu$. At the depth of formation of weak Mn II transitions, the optical depth at this frequency will be large, and Λ is essentially the unit operator. The net rate is therefore

$$R(i \rightarrow j) = -n_j\, A_{ji}\, \left(1 - S^{\mathrm{Ly}\alpha}/S_{ij}\right). \qquad (5)$$

Here the definition of the line source function for the Mn II transition, $S_{ij} = n_j\, A_{ji}/(n_i\, B_{ij} - n_j\, B_{ji})$, has been used. Direct calculation in this work suggests that in an unstratified photosphere, Mn II $\lambda\,6122.4$ forms near $\log \tau_{5000} \approx -0.5$ to -1, depending on the abundance. At these photospheric depths, the Mn II departure coefficients are nearly equal due to strong collisional coupling, and this thermalizes the line source functions to the local Planck function (i.e. $S_{ij} = B_\nu(T_{\mathrm{e}})$). Thus, Ly$\alpha$ fluorescent excitation requires that the Lyα source function *exceed* the local Planck function. If Lyα is thermalized with $S^{\mathrm{Ly}\alpha} = B_\nu(T_{\mathrm{e}})$, the net pumping rate is zero regardless of the number of close wavelength co-incidences with Lyα.

At the depth of formation of multiplet 13, the mean optical depth in Lyα is $\approx 10^{+9.5}$. Using the results of Gayley (1992a, 1992b) to estimate the thermalization length of Lyα in typical late-B photospheres, one finds that Lyα is effectively thermalized with its source function equal to the Planck function at the local kinetic temperature. Thus, the net pumping rate due to Lyα fluorescence is zero. The thermalized radiation field in Lyα will also act maintain the LTE population ratio between the first two hydrogen levels; any postulated interlocked effects (for example, photon loses in Hα, which might be invoked to provide additional population to $n = 2$) will not disturb the thermalization of the Lyα source function in these deep photospheric layers.

5. Conclusions

All of the stars found by W&H to have emission in Mn II multiplet 13 can be interpreted in terms of standard, non-LTE line formation acting in the photosphere. In addition, evidence for the stratification of the manganese abundance profile is particularly strong for HD 186122 (46 Aql) and HD 179761 both of which require manganese to be confined to column masses above $\log(m) \approx -1.5$ to be consistent with the available observations.

Modeling of a wider wavelength range of the Mn II spectrum should provide much tighter constraints on the possible stratification models for HgMn and related stars. In addition, it is important to demonstrate that the weak emission lines of Ti II and Cr II also noted by W&H can be interpreted within the non-LTE framework presented in this letter.

Acknowledgements. I would like to thank J. D. Landstreet for many helpful discussions, and the referees, Glenn Wahlgren and Mike Dworetsky, for their comments. This work is supported by the Natural Sciences and Engineering Research Council of Canada.

References

Adelman, S. J., & Rayle, K. E. 2000, MNRAS, 355, 308
Anders, E., & Grevesse, N. 1989, Geochim. Cosmochim. Acta, 53, 197
Carlsson, M. 1992, in Cool Stars, Stellar Systems, and the Sun, ed. M. S. Giampap, & J. A. Bookbinder, ASP Conf. Ser. 26, 499
Fitzpatrick, E. L., & Massa, D. 1999, ApJ, 525, 1011
Gayley K. G. 1992a, ApJS, 78, 549
Gayley K. G. 1992b, ApJ, 390, 573
Grevesse, N., & Noels, A. 1993, in Origin and Evolution of the Elements, ed. N. Prantzos, E. Vangioni, & M. Cassé (Cambridge University Press), 15
Grigsby, J. A. 1991, ApJ, 380, 606
Grigsby, J. A., Morrison, N. D., & Anderson, L. A. 1992, ApJS, 78, 205
Holt, R. A., Scholl, T. J., & Rosner, S. D. 1999, MNRAS, 306, 107
Sigut, T. A. A. 2001, ApJ, 546, L118
Sigut, T. A. A. 1996, ApJ, 473, 452
Sigut, T. A. A., Landstreet, J. D., & Shorlin, S. L. S. 2000, ApJ, 530, L89
Wahlgren, G. M., & Hubrig, S. 2000, A&A, 2000, 362, L13